Characterization of the Acyl Substrate Binding Pocket of Acetyl-CoA Synthetase[†]

Cheryl Ingram-Smith, Barrett I. Woods, and Kerry S. Smith*

Department of Genetics and Biochemistry, Clemson University, Clemson, South Carolina 29634-0318

Received May 23, 2006; Revised Manuscript Received July 25, 2006

ABSTRACT: AMP-forming acetyl-CoA synthetase [ACS; acetate:CoA ligase (AMP-forming), EC 6.2.1.1] catalyzes the activation of acetate to acetyl-CoA in a two-step reaction. This enzyme is a member of the adenylate-forming enzyme superfamily that includes firefly luciferase, nonribosomal peptide synthetases, and acyl- and aryl-CoA synthetases/ligases. Although the structures of several superfamily members demonstrate that these enzymes have a similar fold and domain structure, the low sequence conservation and diversity of the substrates utilized have limited the utility of these structures in understanding substrate binding in more distantly related enzymes in this superfamily. The crystal structures of the *Salmonella enterica* ACS and *Saccharomyces cerevisiae* ACS1 have allowed a directed approach to investigating substrate binding and catalysis in ACS. In the *S. enterica* ACS structure, the propyl group of adenosine 5′-propylphosphate, which mimics the acyl-adenylate intermediate, lies in a hydrophobic pocket. Modeling of the *Methanothermobacter thermautotrophicus* Z245 ACS (MT-ACS1) on the *S. cerevisiae* ACS structure showed similar active site architecture, and alignment of the amino acid sequences of proven ACSs indicates that the four residues that compose the putative acetate binding pocket are well conserved. These four residues, Ile^{312}, Thr^{313}, Val^{388}, and Trp^{416} of MT-ACS1, were targeted for alteration, and our results support that they do indeed form the acetate binding pocket and that alterations at these positions significantly alter the enzyme's affinity for acetate as well as the range of acyl substrates that can be utilized. In particular, Trp^{416} appears to be the primary determinant for acyl chain length that can be accommodated in the binding site.

AMP-forming acetyl-CoA synthetase [ACS;[1] acetate:CoA ligase (AMP-forming), EC 6.2.1.1] catalyzes the activation of acetate to acetyl-CoA in a two-step reaction (eqs 1a and 1b) involving formation of an acetyl-adenylate enzyme-bound intermediate in the first step (*1*−*4*):

$$E + \text{acetate} + ATP \leftrightarrow E{\cdot}\text{acetyl-AMP} + PP_i \quad (1a)$$

$$E{\cdot}\text{acetyl-AMP} + HSCoA \leftrightarrow E + \text{acetyl-CoA} + AMP \quad (1b)$$

ACS is a member of the adenylate-forming enzyme superfamily that contains three subfamilies: the acyl- and aryl-CoA synthetases, the adenylation domain of nonribosomal peptide synthetases (NRPS), and firefly luciferase (*5*). These enzymes share limited sequence homology, but all catalyze a two-step reaction in which an enzyme-bound acyl-adenylate is formed in the first half-reaction and, for most enzymes in this superfamily, a thioester product is formed from the acyl-adenylate intermediate in the second half-reaction.

Although sequence identity among distant members of the superfamily is low, three conserved signature motifs have been identified (*5*): motif I, **T**[SG]-**S**[G]-**G**-[ST]-**T**[SE]-**G**[S]-X-**P**[M]-**K**-**G**[LF] (residues 266−275 in the *Methanothermobacter thermautotrophicus* MT-ACS1, the subject of this investigation); motif II, **Y**[LWF]-**G**[SMW]-X-**T**[A]-**E** (residues 415−419 in MT-ACS1); and motif III, **Y**[FL]-**R**[KX]-**T**[SV]-**G**-**D** (residues 498−502 in MT-ACS1), in which the boldface residues represent those that predominate at each position, the residues in brackets represent the most common alternative residues observed, and X represents hypervariable positions. Previous investigations into substrate binding and catalysis in this superfamily have focused primarily on conserved motifs I and II (*5*−*10*). The crystal structures of several members of the adenylate-forming enzyme superfamily indicate that these enzymes have a large N-terminal domain and a smaller ∼110 amino acid C-terminal domain with the active site located at the interface between the two domains (*9*, *11*, *12*). The crystal structures of firefly luciferase and other members of the superfamily revealed that motifs I, II, and III are all located on the surface at the domain interface (*11*), supporting a role for these motifs in substrate binding and catalysis. In addition to the signature motifs, ten conserved core sequence motifs have been identified for the nonribosomal peptide synthetases, of which seven are conserved in the acyl-CoA synthetases (*13*−*16*).

The crystal structures of the *Salmonella enterica* ACS (*16*) and *Saccharomyces cerevisiae* ACS1 (*17*) have allowed a directed approach to investigating substrate binding and catalysis in ACS. The *S. cerevisiae* ACS1 was crystallized in the presence of ATP but in the absence of acetate (*17*).

[†] Financial support by the NIH (Award GM69374-01A1 to K.S.S.), South Carolina Experiment Station (Project SC-1700198 to K.S.S.), and Clemson University. B.I.W. was supported by the NIH-NSF Bioengineering Institute in Biomaterials Science and Engineering (Award 0234082).

* Corresponding author. Phone: 864-656-6935. Fax: 864-656-0393. E-mail: kssmith@clemson.edu.

[1] Abbreviations: ACS, acetyl-CoA synthetase; MT-ACS1, *Methanothermobacter thermautotrophicus* Z245 ACS1; SACS, short/medium-chain acyl-CoA synthetase.

10.1021/bi061023e CCC: $33.50
Published on Web 09/02/2006

Its C-terminal domain is positioned away from the N-terminal domain in the conformation thought to be responsible for catalysis of the first step of the reaction (*17*). The *S. enterica* ACS enzyme was crystallized in the presence of CoA and adenosine 5′-propylphosphate, an inhibitor that mimics the acetyl-adenylate intermediate (*7*, *18*). In this structure, the C-terminal domain is rotated 140° toward the N-terminal domain for catalysis of the second step of the reaction (*16*). The propyl group of the adenosine 5′-propylphosphate inhibitor is located in a position similar to that of the phenylalanine substrate in the structure of PheA, the phenylalanine adenylation domain of the NRPS gramicidin synthetase 1. Thus, although ACS adopts this conformation after formation of the acyl-adenylate intermediate and is poised to catalyze the second half-reaction, the position of the propyl group likely approximates the position of the acetate substrate of ACS.

In this paper, we report the identification of the acetate binding pocket in the *M. thermautotrophicus* ACS1 (designated as MT-ACS1). Our characterization of this enzyme (*30*) has shown that MT-ACS1 has a higher turnover rate but similar affinity for substrates as the *S. enterica* ACS (J. Thurman, C. Ingram-Smith, K. Zimowski, and K. S. Smith, manuscript in preparation), making it an excellent candidate for studies on substrate binding. Through inspection of the *S. enterica* ACS structure, modeling of the *M. thermautotrophicus* MT-ACS1 on the *S. cerevisiae* ACS1 and *S. enterica* ACS structures, and alignment of ACS sequences, we have identified four residues that form the putative acetate binding pocket. These residues have been targeted for alteration to investigate their roles in acetate binding and catalysis. The results support that Ile^{312}, Thr^{313}, Val^{388}, and Trp^{416} do indeed form the acetate binding pocket and that replacements at these positions significantly alter the enzyme's affinity for acetate as well as the range of acyl substrates that can be utilized.

EXPERIMENTAL PROCEDURES

Materials. Chemicals were purchased from VWR Scientific Products, Fisher Scientific, or Sigma Chemicals. Oligonucleotides for site-directed mutagenesis were purchased from Integrated DNA Technologies. IRD-700 and IRD-800 labeled oligonucleotides for DNA sequencing were purchased from Li-Cor Biosciences or MWG Biotech.

Site-Directed Mutagenesis. Site-directed mutagenesis of the gene encoding the *M. thermautotrophicus* Z245 MT-ACS1 was performed using the QuikChange site-directed mutagenesis kit (Stratagene) according to the manufacturer's instructions. Mutagenic primers were 30−40 nucleotides in length with the altered base(s) located at the middle of the sequence. The sequence alterations were confirmed by Li-Cor bidirectional sequencing at the Nucleic Acid Facility at Clemson University using the Thermo sequenase primer cycle sequencing kit (GE Healthcare).

Analysis of Short-Chain Acyl-CoA Synthetase Sequences. Searches of the nonredundant sequence databases at the National Center for Biotechnology Information (NCBI) were performed with the BLASTp and tBLASTn programs (*19*, *20*) using the MT-ACS1 sequence as the query. Sequences were aligned by Clustal X (*21*) using a Gonnet PAM 250 weight matrix with a gap opening penalty of 10.0 and a gap extension penalty of 0.05. Sequence identity between MT-ACS1 and other SACSs was determined using the BLAST2 pairwise sequence alignment program available at NCBI (http://www.ncbi.nlm.nih.gov/blast/bl2seq/wblast2.cgi).

Heterologous Production and Purification of MT-ACS1 Variants. Wild-type MT-ACS1 and its variants were heterologously produced in *Escherichia coli* Rosetta Blue(DE3) (Novagen) as described elsewhere (*30*). Cells were grown at 37 °C to an absorbance of 0.4−0.6 at 600 nm, and production of the wild-type enzyme or enzyme variant was induced by the addition of IPTG to a final concentration of 0.5 mM. Cells were incubated at 200 rpm overnight at ambient temperature and harvested. Cell-free extract was prepared by resuspending the cells in buffer A [25 mM Tris (pH 7.5)] and passing them twice through a French pressure cell at 138 MPa. The extracts were clarified by ultracentrifugation, and the supernatant was subjected to column chromatography. Cell-free extracts were applied to a Q-Sepharose fast-flow anion-exchange column (GE Healthcare) which was developed with a linear gradient from 0 to 1 M KCl in buffer A [25 mM Tris (pH 7.5)]. Appropriate fractions as determined by SDS−PAGE and activity assays were pooled and diluted with 0.5 volume of buffer B [25 mM Tris (pH 7.0)] containing 2 M ammonium sulfate and applied to a Phenyl-Sepharose fast-flow hydrophobic interaction column (GE Healthcare) which was developed with a gradient from 0.7 to 0 M ammonium sulfate in buffer B. Fractions containing the purified variant enzyme were pooled and dialyzed against buffer B and concentrated to >1 mg/mL. An additional Source Q (GE Healthcare) anion-exchange chromatography step was added if the variant enzyme was not sufficiently pure after the first two steps. The Source Q column was developed with a linear gradient of 0−1 M KCl in buffer B, and the purified enzyme was dialyzed and concentrated. Aliquots of each purified protein were stored at −20 °C. Protein concentration was determined by the Bradford method (*22*).

Enzymatic Assays for ACS Activity. Enzymatic activity was determined by monitoring acyl-CoA formation using the hydroxamate reaction (*23*, *24*), in which activated acyl groups are converted to an acyl-hydroxamate and subsequently to a ferric hydroxamate complex that is detected spectrophotometrically at 540 nm. The standard reactions contained 100 mM Tris (pH 7.5), 600 mM hydroxylamine hydrochloride (pH 7.0), and 2 mM glutathione (reduced form) in addition to the three substrates (HSCoA, MgATP, and acyl substrate) in a 300 μL reaction volume. In all cases, the Mg^{2+} and ATP were equimolar concentrations. The reactions were performed at 65 °C, the optimal temperature for this enzyme (*30*), and terminated by the addition of two volumes of stop solution (1 N HCl, 5% trichloroacetic acid, 1.25% $FeCl_2$).

For determination of apparent kinetic parameters, the concentration of one substrate (acyl substrate, HSCoA, or MgATP) was varied and the other two substrates were held constant at saturating level (generally 10 times the K_m value for those substrates). Concentrations for the varied substrate generally ranged from 0.2 to 5−10 times the K_m value. In cases in which the acyl substrate was soluble in ethanol but not water, the final concentration of ethanol in the reaction was kept constant at 2%. This concentration was determined to have minimal effect on enzymatic activity (data not shown). The steady-state parameters k_{cat} and k_{cat}/K_m and their

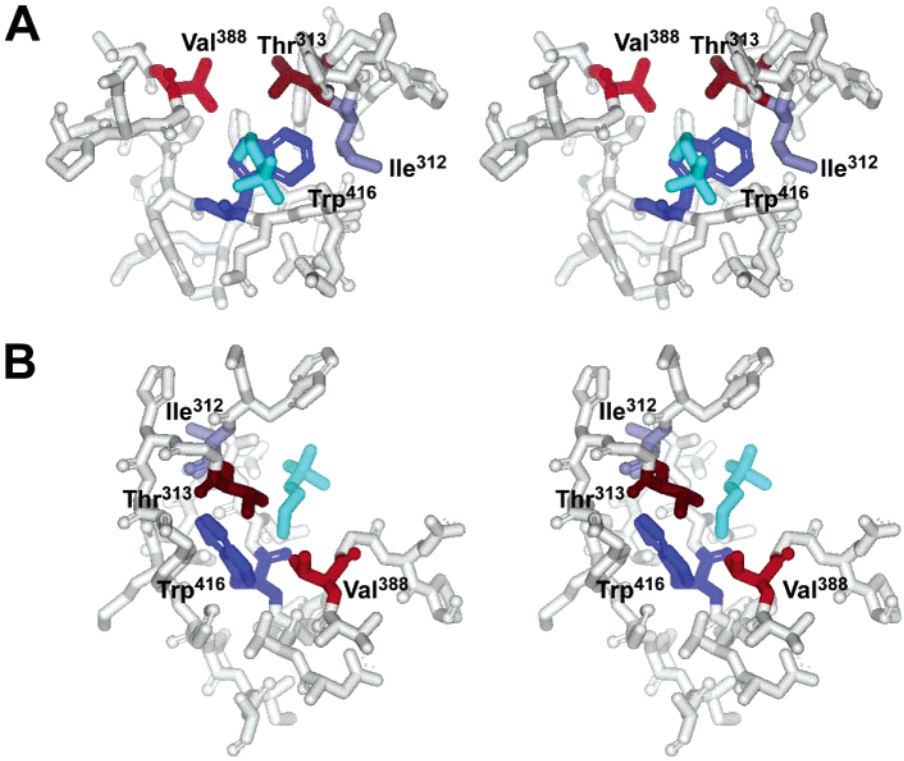

FIGURE 1: The putative acetate pocket of wild-type MT-ACS1. MT-ACS1 was modeled on the *S. enterica* ACS structure using Accelrys DS Modeler 1.1, and the stereo image of the putative active site acetate binding pocket was created using DS ViewerPro 5.0. Residues within 10 Å of the propyl moiety of the propylphosphate group of the adenosine 5′-propylphosphate mimic of the acetyl-adenylate intermediate are shown. Ile^{312} is shown in purple, Thr^{313} in magenta, Val^{388} in red, and Trp^{416} in blue. The propylphosphate group is shown in aqua. Note that all residues depicted in this structure are shown in the alignment in Figure 2. (A) Front view in which the propyl group is directed into the pocket. (B) Side view showing steric hindrance between the propyl group and Trp^{416}.

standard errors were determined using nonlinear regression to fit the data to the Michaelis−Menten equation using Kaleidagraph (Synergy Software). The enzyme variants followed Michaelis−Menten kinetics for all substrates. The wild-type enzyme showed inhibition above 0.5 mM HSCoA, in which case the kinetic parameters for the other substrates were determined in the presence of 0.5 mM HSCoA and must be considered apparent values (*30*).

Molecular Mass Determination. The native molecular masses of the variants were determined by gel filtration chromatography using a Superose 12 gel filtration column (GE Healthcare) calibrated with chymotrypsinogen (25 kDa), ovalbumin (43 kDa), albumin (67 kDa), aldolase (158 kDa), catalase (232 kDa), ferritin (440 kDa), and blue dextran (2000 kDa). The column was preequilibrated with 50 mM Tris (pH 7.5) containing 150 mM KCl and developed at a flow rate of 0.5 mL/min.

Modeling the MT-ACS1 Structure and the Putative Acetate Binding Pocket. The *M. thermautotrophicus* MT-ACS1 structure was modeled on both the *S. enterica* ACS structure (PDB ID: 1PG4) and the *S. cerevisiae* ACS1 structure (PDB ID: 1RY2) using DS Modeler (Accelrys) using the standard parameters built into the program. The structures were visualized with DS Visualizer (Accelrys) and DS Viewer Pro 5.0 (Accelrys). The MT-ACS1 models were visually compared to the *S. enterica* and *S. cerevisiae* ACS structures to ensure that there were no major structural anomalies.

RESULTS

Identification of the Putative Acetate Binding Pocket. The crystal structure of the *S. enterica* ACS was solved in the presence of CoA and adenosine 5′-propylphosphate (*16*), a mimic of the enzyme-bound acetyl-AMP intermediate (*7*, *18*). Inspection of the *S. enterica* ACS structure revealed a hydrophobic pocket consisting of Val^{310}, Val^{386}, and Trp^{414} in proximity to the propyl group of adenosine 5′-propylphosphate. In addition, Thr^{311} is located in the immediate vicinity and appears to form a wall of this pocket. The propyl group of the inhibitor may provide an approximation for the position of acetate bound in the active site; therefore, this hydrophobic pocket may thus represent the acetate binding pocket of ACS.

The *M. thermautotrophicus* Z245 MT-ACS1 was modeled on the *S. enterica* ACS and *S. cerevisiae* ACS1 structures. Both of these models were highly analogous to the structures on which they were based (data not shown). The MT-ACS1 model of the *S. enterica* ACS structure indicates that Ile^{312}, Thr^{313}, Val^{388}, and Trp^{416} form a hydrophobic pocket positioned similarly to that formed by Val^{310}, Thr^{311}, Val^{386}, and Trp^{414} of the *S. enterica* enzyme, In this model, the propyl group of adenosine 5′-propylphosphate points directly into the pocket toward Trp^{416} and is surrounded on three sides by Ile^{312}, Thr^{313}, and Val^{388} (Figure 1). Thus, these four residues were suitable candidates for site-directed replacement to determine whether alteration of this pocket influenced acetate affinity and catalysis.

The residues that form the putative acetate binding pocket would be expected to be highly conserved among the ACSs. For short/medium-chain acyl-CoA synthetases (SACS) that show a preference for acyl substrates other than acetate, it would be expected that one or more conserved residues that form the acetate binding pocket in ACS would be replaced

	312/313	388	416
MT-ACS1	307 ADIGW**IT**GHSY 317	387 T**V**GEP 391	413 DTW**W**QTETGMHLIA 426
S.enterica ACS	305 ADVGW**VT**GHSY 315	385 S**V**GEP 389	411 DTW**W**QTETGGFMIT 424
Yeast ACS1	361 GDIGW**IT**GHTY 371	441 S**V**GEP 445	467 DTY**W**QTESGSHLVT 480
Yeast ACS2	319 GDVGW**IT**GHTY 329	399 S**V**GEP 403	425 DTM**W**QTESGSHLIA 438
M.concilii ACS	329 ADIGW**VT**GHSY 339	409 S**V**GEP 413	435 DTW**W**QTETGTFLNS 448
H.marismortui ACS	314 ADIGW**IT**GHSY 324	394 T**V**GEP 398	420 DTW**W**QTETGGMMIT 433
P.aerophilum ACS	320 ADIGW**VT**GHSY 330	400 S**V**GEP 404	426 STW**W**MTETGGIVIS 439
S.enterica PCS	281 SDIGW**VV**GHSY 291	361 L**A**GEP 365	387 DNY**W**QTESGWPIMA 400
Human SA	276 SDTGW**AK**SAWS 286	351 S**A**GEP 355	377 EGY**G**QTETV-LICG 389
Human MACS1	267 SDSGW**IV**ATIW 277	342 T**G**GEV 346	368 ENY**G**QSETG-LICA 380
E.coli FadK	236 APLGH**AT**GFLH 246	310 C**G**GTT 314	336 SVY**G**STESSPHAVV 349

FIGURE 2: Partial ACS/SACS sequence alignment. Amino acid sequences were aligned using Clustal X (*21*). The residues represented in the structure in Figure 1 are shown. Residues proposed to interact with acetate are shaded in gray. For brevity, only the sequences of MT-ACS1 (gi:82541817) and several proven SACSs are included. Percent identity/similarity between MT-ACS1 and the SACS sequences are as follows: *S. enterica* ACS (gi:16767525), 49%/66%; yeast ACS1 (gi:6319264), 43%/63%; yeast ACS2 (gi:6323182), 45%/62%; *Methanosaeta concilii* ACS (gi:113312), 49%/69%; *Haloarcula marismortui* ACS (gi:55379786), 44%/65%; *Pyrobaculum aerophilum* ACS (gi:18313648), 52%/73%; *S. enterica* PCS (gi:16763751), 39%/59%; human SA (gi:14779921), 29%/47%; human MACS1 (gi:16418449), 30%/46%; *E. coli* FadK (gi:3220009), 26%/42%.

Table 1: Kinetic Parameters for the Ile^{312} and Thr^{313} MT-ACS1 Variant Enzymes

enzyme	substrate[a]	K_m[b] (mM)	k_{cat}[b] (s^{-1})	k_{cat}/K_m[b] (s^{-1} mM^{-1})
wild-type	acetate	3.5 ± 0.1	65.4 ± 0.3	18.6 ± 0.5
	propionate	36.5 ± 1.9	46.3 ± 0.7	1.3 ± 0.04
Ile^{312}Ala	acetate	24.6 ± 0.8	30.4 ± 0.2	1.24 ± 0.03
	propionate	73.1 ± 1.1	18.2 ± 0.1	0.25 ± 0.004
	butyrate	136.4 ± 3.5	0.47 ± 0.004	0.0034 ± 0.0001
Thr^{313}Val	acetate	0.46 ± 0.009	3.4 ± 0.03	7.3 ± 0.07
	propionate	4.5 ± 0.06	5.9 ± 0.01	1.31 ± 0.02
Thr^{313}Lys	acetate	596 ± 34	1.9 ± 0.05	<0.01
	propionate	*c*	*c*	*c*

[a] Activity was detected only with the substrates shown and was not detected with branched-chain substrates. [b] Kinetic parameters were determined at saturating concentrations of the cosubstrates and are therefore considered apparent. [c] Activity was detected but was too low for determination of kinetic parameters.

with smaller residues in order to increase the size of the pocket to accommodate longer straight-chain acyl substrates or the bulkier branched-chain acyl substrates. Indeed, alignment of the sequences of proven ACSs and SACSs bears out these predictions (Figure 2).

The SACSs shown in Figure 2 show different substrate preferences, ranging from acetate and propionate for ACS and propionyl-CoA synthetase (PCS) (*7*) to isobutyrate for Sa and octanoate for MACS1 (*25*). The acyl substrate preference has not yet been determined for FadK, a SACS from *E. coli*, but this enzyme has been shown to utilize substrates ranging from hexanoate to decanoate (*26*). Thr^{313}, Val^{388}, and Trp^{416} of MT-ACS1 are completely conserved among the ACSs, and Ile^{312} is well conserved. SACSs that utilize these longer chain acyl substrates do indeed have alterations at one or more equivalent positions (Figure 2). Perhaps the most interesting observations from the alignment in Figure 2 are the replacements at Val^{388} and Trp^{416}. Val^{388} is replaced by Ala in PCS and Sa but by the smaller residue Gly in MACS1 and FadK, which utilize longer acyl substrates. Trp^{416} is conserved in the ACSs and PCS but is universally replaced by Gly in SACSs that utilize longer acyl substrates.

Purification of Wild-Type and Variant ACSs. Each of the four residues (Ile^{312}, Thr^{313}, Val^{388}, and Trp^{416}) postulated to form part of the acetate binding pocket of the *M. thermautotrophicus* MT-ACS1 was individually subjected to site-directed replacement with amino acid residues present in other SACSs (Figure 2). The variants displayed behavior similar to that of the wild-type enzyme in each chromatographic step, the subunit molecular masses were indistinguishable from that of the wild-type enzyme as determined by SDS−PAGE (data not shown), and gel filtration chromatography indicated that the variants were dimeric, as for the wild-type enzyme. These results suggest that the purified variants had not undergone major structural changes.

Kinetic Parameters for the Ile^{312} and Thr^{313} Variants. The kinetic constants for acyl substrate utilization by the wild-type enzyme and the Ile^{312} and Thr^{313} variants are shown in Table 1. Although acetate was the preferred substrate over propionate for the Ile^{312}Ala variant, as indicated by the higher catalytic efficiency (k_{cat}/K_m), the difference in catalytic efficiency with these two substrates is only 5.0-fold, as compared to a 14.3-fold difference in the catalytic efficiency of the wild-type enzyme with acetate versus propionate. Whereas the wild-type enzyme can only utilize acetate and propionate as the acyl substrate, this variant has gained the ability to utilize butyrate as a substrate, albeit a poor one, but cannot use longer acyl substrates or branched-chain acyl substrates.

The Thr^{313}Val variant demonstrated a 7−8-fold greater affinity for acetate and propionate as compared to the wild-type enzyme. In fact, the K_m for propionate for the Thr^{313}-Val variant was only slightly higher than that observed for the wild-type enzyme with acetate. As for the Ile^{312}Ala variant, the Thr^{313}Val variant showed weaker preference for acetate versus propionate than observed for the wild-type enzyme (5.6-fold as compared to 14.3-fold). The Thr^{313}Lys variant proved to be a poor enzyme with a weak affinity for acetate and over a 5000-fold reduction in catalytic efficiency

Table 2: Kinetic Parameters for Val[388] MT-ACS1 Variant Enzymes

enzyme	substrate[a]	K_m[b] (mM)	k_{cat}[b] (s^{-1})	k_{cat}/K_m[b] (s^{-1} mM^{-1})
Val[388]Ala	acetate	13.2 ± 0.6	36.2 ± 0.4	2.7 ± 0.1
	propionate	4.1 ± 0.2	13.2 ± 0.1	3.2 ± 0.2
	butyrate	151.9 ± 18.3	1.56 ± 0.05	0.01 ± 0.001
Val[388]Gly	acetate	164.4 ± 8.5	31.9 ± 0.5	0.2 ± 0.01
	propionate	128.6 ± 2.0	6.0 ± 0.04	0.05 ± 0.001

[a] Activity was detected only with the substrates shown and was not detected with branched-chain substrates. [b] Kinetic parameters were determined at saturating concentrations of the cosubstrates and are therefore considered apparent.

as compared to the wild-type enzyme. This enzyme had very weak but detectable activity with propionate that was too low for determination of kinetic parameters. Neither of the Thr[313] variants was able to utilize butyrate or branched-chain substrates.

Kinetic Parameters for the Val[388] Variants. Kinetic parameters for the Val[388] variants are shown in Table 2. Alteration of Val[388] to Ala resulted in a shift in substrate preference from acetate to propionate. The K_m for acetate increased 3.8-fold relative to that of the wild-type enzyme (Table 2) whereas that for propionate decreased 8.9-fold. Interestingly, the catalytic efficiency with propionate as the substrate was increased in the variant relative to that observed for the wild-type enzyme, and in fact, the variant showed a slightly higher catalytic efficiency with propionate than with acetate. Unlike the wild-type enzyme, this variant was able to utilize butyrate, although this was a poor substrate. Longer acyl substrates and branched-chain substrates could not serve as a substrate for this variant.

The Val[388]Gly variant had a 47-fold higher K_m for acetate but only a 2-fold lower turnover rate as compared to the wild-type enzyme. The effect of the alteration on the K_m for propionate was less dramatic, but the overall catalytic efficiency with propionate was 26-fold reduced relative to the wild-type enzyme. Overall, the variant showed only a 4-fold preference for acetate as the substrate as compared to a 14.3-fold preference for the unaltered enzyme. Unlike the Val[388]Ala variant, this variant was unable to utilize butyrate.

Kinetic Parameters for the Trp[416] Variants. A Trp[416]Gly alteration had a very dramatic effect on MT-ACS1 substrate range and preference. Whereas the wild-type enzyme can utilize only acetate and propionate but not larger substrates such as butyrate or valerate or branched-chain acyl substrates, the substrates utilized by the Trp[416]Gly variant ranged from the two-carbon acetate to the eight-carbon octanoate. The enzyme was also able to utilize the branched-chain substrates 2-, 3-, and 4-methylvalerate (Table 3) but was unable to utilize 2-methylpropionate, 2-methylbutyrate, and 3-methylbutyrate. The lowest K_m values were observed with hexanoate and 4-methylvalerate and were less than 2.2-fold higher than the K_m of the wild-type enzyme for acetate.

The highest turnover rate for the Trp[416]Gly variant was observed with acetate; however, the high K_m value made this a catalytically inefficient substrate. Although the k_{cat} values generally decreased as the substrate length increased, the K_m values also decreased for longer chain substrates. Thus, the Trp[416]Gly alteration shifted substrate preference from acetate, with a k_{cat}/K_m of only 0.26 s^{-1} mM^{-1}, to valerate, hexanoate, and 4-methylvalerate, with 3.7−5.4-fold higher k_{cat}/K_m values.

Table 3: Kinetic Parameters for the Trp[416]Gly MT-ACS1 Variant Enzyme

substrate[a]	K_m[b] (mM)	k_{cat}[b] (s^{-1})	k_{cat}/K_m[b] (s^{-1} mM^{-1})
straight chain			
acetate	132.1 ± 9.9	33.7 ± 0.8	0.26 ± 0.01
propionate	188.8 ± 1.2	19.2 ± 0.1	0.10 ± 0.005
butyrate	39.2 ± 0.9	10.8 ± 0.1	0.27 ± 0.005
valerate	11.1 ± 0.5	11.9 ± 0.2	1.07 ± 0.04
hexanoate	6.1 ± 0.09	5.9 ± 0.02	0.96 ± 0.01
heptanoate	10.2 ± 0.4	7.3 ± 0.12	0.72 ± 0.02
octanoate	18.1 ± 0.9	3.3 ± 0.1	0.18 ± 0.004
branched chain			
2-methylvalerate	*c*	*c*	*c*
3-methylvalerate	29.2 ± 2.1	0.67 ± 0.02	0.023 ± 0.001
4-methylvalerate	7.6 ± 0.3	10.9 ± 0.02	1.42 ± 0.02

[a] Activity was detected only with the straight- and branched-chain substrates shown. [b] Kinetic parameters were determined at saturating concentrations of the cosubstrates and are therefore considered apparent. [c] Activity was detected but was too low for determination of kinetic parameters.

Table 4: K_m Values for ATP and CoA for the MT-ACS1 Variant Enzymes

enzyme	K_m(MgATP)[b] (mM)	K_m(CoA)[b] (mM)
wild-type[a]	3.3 ± 0.2	0.19 ± 0.003
Ile[312]Ala	6.6 ± 0.2	0.18 ± 0.001
Thr[313]Val	0.65 ± 0.04	0.70 ± 0.02
Thr[313]Lys	3.4 ± 0.1	*c*
Val[388]Ala	2.6 ± 0.1	0.35 ± 0.02
Val[388]Gly	4.0 ± 0.3	0.18 ± 0.005
Trp[416]Gly	2.3 ± 0.06	0.43 ± 0.028

[a] The wild-type enzyme showed inhibition above 0.5 mM CoA. [b] Kinetic parameters were determined at saturating concentrations of the cosubstrates and are therefore considered apparent. [c] Enzyme does not utilize CoA.

ATP and CoA Utilization by the MT-ACS1 Variants. The kinetic constants for ATP and CoA shown in Table 4 for the wild-type and variant enzymes were determined using the acyl substrate that provided the highest catalytic efficiency for each enzyme. Except for the Thr[313]Val and Thr[313]Lys variants, the K_m values for ATP and CoA showed less than 3-fold difference for the variants as compared to the wild-type enzyme. These results support that the overall structure of the active site is not altered in the Ile[312], Val[388], and Trp[416] variants.

With the Thr[313]Lys variant, activity was detected using the hydroxamate assay even in the absence of CoA. As the hydroxamate reaction is not specific for detection of acetyl-CoA but instead detects activated acyl groups, production of an activated acetyl group in the absence of CoA suggests that the Thr[313]Lys variant may release the acetyl-adenylate intermediate and cannot catalyze the second step of the ACS reaction. For wild-type MT-ACS1, no product was detected

in the absence of CoA using the hydroxamate assay (data not shown), indicating that the enzyme-bound acyl-adenylate intermediate is not detected by the hydroxamate reaction. Inorganic pyrophosphate was detected as one of the products of the reaction catalyzed by the Thr^{313}Lys variant using an inorganic pyrophosphatase assay (data not shown), suggesting that this variant catalyzes the first step of the reaction to form the expected products.

DISCUSSION

Although members of the acyl-adenylate-forming enzyme superfamily all catalyze mechanistically similar two-step reactions, they share little identity and similarity in amino acid sequence with the exception of a few signature and core motifs. The crystal structures of several diverse members of this superfamily have revealed that these enzymes adopt a similar two-domain structure in which the active site resides in the cleft between the N- and C-terminal domains. These enzymes are all thought to adopt two different conformations in which alternation of the C-terminal domain after catalysis of the first step of the reaction restructures the active site for catalysis of the second half-reaction.

Despite the structural similarities, the diversity of substrates and the divergence in primary sequence among enzymes in this superfamily have limited the utility of distantly related structures in identifying primary determinants for binding of the acyl substrate in ACS and other short-chain acyl-CoA synthetases. The structures of the *S. enterica* ACS and the *S. cerevisiae* ACS1 provide direct insight into the active site residues of ACS. Although the yeast ACS structure does not include bound acetate, a comparison of the two ACS structures indicates that the positions of the residues located in the putative acetate binding pocket remain relatively unaffected by domain alternation.

The location of the propyl group of the adenosine 5′-propylphosphate present in the structure of the *S. enterica* ACS provides an approximation of where the acetate binding pocket resides in ACS (*16*). However, our kinetic characterization of the *Salmonella typhimurium* ACS, which has the identical sequence as the *S. enterica* ACS, indicated that the activity of this enzyme is prohibitively low for characterization of enzyme variants with greatly reduced activity (J. Thurman, C. Ingram-Smith, K. Zimowski, and K. S. Smith, manuscript in preparation). Sequence alignment and modeling of MT-ACS1 on the *S. enterica* and *S. cerevisiae* ACS structures suggest that the active sites of these enzymes are highly conserved. Thus, MT-ACS1 was a suitable enzyme for our studies on substrate binding in ACS using information derived from the ACS crystal structures. Furthermore, the higher turnover rate of MT-ACS1 allowed variants with greatly reduced activity to be kinetically characterized to determine whether the effect of the alteration is on substrate affinity, catalysis, or both.

In this study, four residues that comprise a hydrophobic pocket in the vicinity of the propyl group of the adenosine 5′-propylphosphate in the MT-ACS1 model (Figure 1) were targeted for site-directed replacement to determine whether they do indeed form the acetate binding site. Each of these residues was individually altered in order to examine their individual contributions to acyl substrate binding in terms of both substrate affinity and the size of the acyl substrate that can be accommodated. The high catalytic activity of MT-ACS1 has allowed variants with low activity to be characterized to determine whether the alteration affects substrate affinity, catalysis, or both.

Trp^{416} and Val^{388} were found to have the strongest influence on acyl substrate utilization. Alteration of Trp^{416} proved to have a dramatic effect on both substrate range and substrate preference for MT-ACS1. ACSs and PCSs have Trp at the position equivalent to Trp^{416} of MT-ACS1 (Figure 2). Enzymes such as Sa, MACS1, and FadK that show a preference for longer acyl substrates have Gly at this position instead of Trp (Figure 2). Remarkably, the Trp^{416}Gly variant was able to utilize substrates as large as octanoate and also utilized branched-chain acyl substrates in addition to straight-chain acyl substrates (Table 3).

The Trp^{416} variant had weak affinity for acetate and propionate, the only two acyl substrates utilized by the wild-type enzyme. Instead, the enzyme had the strongest affinity for hexanoate, heptanoate, and valerate and showed the highest catalytic efficiency with the branched-chain substrate 4-methylvalerate, followed by valerate, hexanoate, and heptanoate. Thus, it appears that removal of the Trp side chain from the hydrophobic pocket is sufficient to enlarge the pocket to accommodate longer substrates in preference to acetate and propionate. A model of the Trp^{416}Gly variant (Figure 3) is consistent with this. In this model, the propylphosphate group (shown in aqua) was increased in length by two methylenes to mimic binding of valerate. It is readily apparent that removal of the bulky side chain allows the pocket to accommodate a longer substrate without steric hindrance as would be observed in the wild-type enzyme.

It should be noted that the overall catalytic efficiency of the wild-type enzyme is 13-fold higher than that observed for the Trp^{416}Gly variant with its best substrate, 4-methylvalerate. However, the turnover rate of the variant with acetate is reduced only 2-fold from the wild-type enzyme, indicating that catalysis itself is not significantly impaired. This suggests that although the variant can bind longer substrates, the overall architecture of the active site is not optimal for utilization of substrates larger than acetate or propionate.

Alteration of Val^{388} to Ala, as seen in PCS and Sa (which utilize propionate and 2-methylpropionate, respectively) (Figure 2), transformed MT-ACS1 into an enzyme with a slight preference for propionate over acetate (Table 2). The turnover rate of this variant was higher with acetate than with propionate, but the decreased affinity for acetate and increased affinity for propionate rendered the overall catalytic efficiency better with propionate. In addition, this alteration allowed the variant to use butyrate, unlike for the wild-type enzyme. The Val^{388}Gly MT-ACS1 variant had a reduced affinity for acetate and propionate and a poor overall catalytic efficiency with either substrate.

Although the Val^{388}Ala replacement has altered the substrate preference of MT-ACS1 from acetate to propionate, this enzyme variant is not an effective PCS. The *S. enterica* PCS (*7*) shows a strong preference for propionate over acetate, in terms of both affinity (85-fold) and catalytic efficiency (86.5-fold). The Val^{388}Ala MT-ACS1 variant has only a slightly higher catalytic efficiency with propionate than acetate and only 3-fold better affinity for propionate. Furthermore, this alteration decreased the catalytic efficiency 5.8-fold relative to the wild-type enzyme. Although both the

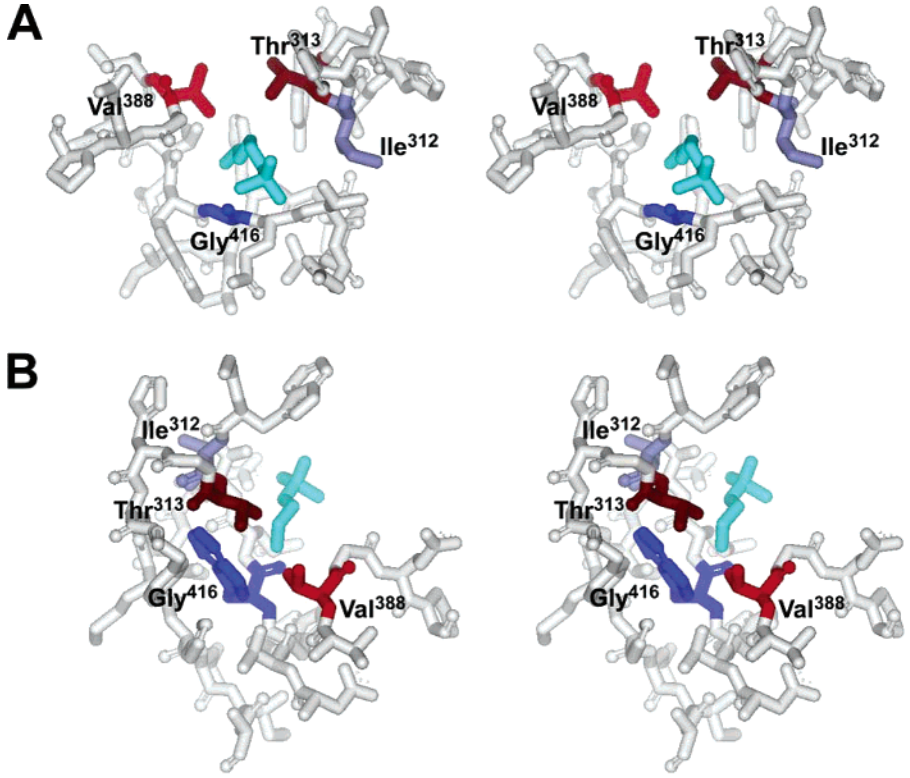

FIGURE 3: The acyl substrate binding pocket of the MT-ACS1 $Trp^{416}Gly$ variant. The variant was modeled on the *S. enterica* ACS structure using Accelrys DS Modeler 1.1, and the stereo image of the putative acyl substrate binding pocket was created using DS ViewerPro 5.0. The propylphosphate group was lengthened by two methylene groups to mimic binding of valerate. Residues within 10 Å of the valeryl moiety are shown. Ile^{312} is shown in purple, Thr^{313} in magenta, Val^{388} in red, and Trp^{416} in blue. The propylphosphate group is shown in aqua. (A) Front and (B) side views similar to those shown in Figure 1.

Val^{388}Ala MT-ACS1 variant and PCS can utilize butyrate, it is a very poor substrate for each.

PCS and Sa, which utilize propionate and 2-methylpropionate, respectively, have Ala in the equivalent position to Val^{388} of MT-ACS1. FadK and MACS1 utilize longer acyl substrates such as hexanoate and octanoate and have Gly in place of Val at this position (Figure 2). The results observed with the Val^{388}Ala variant suggest that reducing the size of the side chain at this position in MT-ACS1 lengthens the hydrophobic pocket to allow slightly longer substrates to be accommodated. However, replacement with Gly likely introduces too much flexibility to the architecture of the pocket, resulting in poor substrate affinity and catalytic efficiency.

Alterations at Thr^{313} proved to be quite interesting. The Thr^{313}Val variant had a very strong affinity for acetate and propionate relative to the wild-type enzyme (Table 1). The fact that the affinity for both of these substrates increased by a similar degree but the substrate range was not affected suggests that replacement of Thr with the hydrophobic residue Val served to increase the overall hydrophobicity of the pocket without greatly altering the shape or size. The increased hydrophobicity of the pocket may also account for the decreased catalytic rate in that it may be more difficult for the enzyme to release the acetyl-CoA product due to stronger hydrophobic interactions.

Replacement of Thr^{313} with Lys, the residue present at the equivalent position in Sa (Figure 2), gave a very unexpected result. The activity of this variant was the same in the presence or complete absence of CoA (Table 4 and data not shown). The hydroxamate assay used in these investigations detects free activated acyl groups such as acetyl-CoA, acetyl phosphate, and acetyl-AMP. Wild-type MT-ACS1 has no detectable activity in the absence of CoA (data not shown), indicating that the enzyme-bound intermediate is not detected by this assay. The Thr^{313}Lys variant not only produces an activated acyl product detectable by the hydroxamate assay but also produces inorganic pyrophosphate, a product of the first step of the reaction. These results suggest that this variant catalyzes the first step of the reaction but releases the acetyl-adenylate intermediate, making the enzyme unable to catalyze the second step of the reaction.

An Ile^{312}Ala alteration in MT-ACS1 had the least effect on substrate utilization of the four residues targeted in this investigation. This replacement allowed the enzyme to utilize butyrate; however, the affinity, turnover rate, and overall catalytic efficiency with this substrate were low (Table 1). The variant had a reduced affinity for acetate and propionate but the turnover rate was only reduced 2−3-fold. The effect on overall catalytic efficiency was most noticeable for acetate and less so for propionate. That alteration of Ile^{312} did not have as great an effect on substrate binding and catalysis as observed for other alterations was not completely unexpected, as this position is the least conserved of the four positions investigated.

Acetate is bound in ACS in a similar position as observed for phenylalanine in the PheA structure, the aryl acid 2,3-dihydroxybenzoate in the DhbE structure, and 4-chlorobenzoate in the 4-chlorobenzoate:CoA ligase/synthetase (CBAL) (*9*, *12*, *16*, *27*), all of which are members of the adenylate-forming enzyme superfamily along with firefly luciferase. PheA, DhbE, CBAL, and luciferase all have Gly at the

position equivalent to Trp^{416} of MT-ACS1 and Ala or Gly at the position equivalent to Val^{388} (*27*), suggesting that these residues play a role in determining substrate utilization for all members of the enzyme superfamily. Both of these residues are positioned in the substrate binding pocket in each of the crystal structures. Replacement of Trp with Gly and Val with either Ala or Gly thus appears to be necessary for these other enzymes to accommodate their respectively larger substrates. Gulick et al. (*27*) have suggested that it is the presence of Trp instead of Gly in ACS and PCS that distinguishes enzymes that utilize small acyl substrates from other family members. Our results confirm this but indicate that the residue at the position equivalent to Val^{388} of MT-ACS1 also plays an important role in distinguishing the size of the acyl substrate.

Although the substrate binding pockets for acetate, phenylalanine, 2,3-dihydroxybenzoate, and 4-chlorobenzoate have been identified in the crystal structures of ACS, PheA, DhbE, and CBAL, respectively, very little has been done experimentally to determine the function of residues within these pockets in determining substrate specificity. In the 4-coumarate:CoA ligase 1 isozyme 4CL1 from soybean, alteration of Gly^{337} (the equivalent to Trp^{416} of MT-ACS1) to Ala resulted in loss of activity of this enzyme with 4-coumarate, the highly ring-substituted cinnamate, and other differently ring-substituted cinnamate substrates (*28*). Furthermore, mutations in a ten-residue region immediately surrounding Gly^{337} also greatly reduced activity with the six substrates tested (*28*). From these experimental results for 4CL1 and the structure of the related enzyme CBAL, Gulick et al. suggest that the aryl-acid pocket residues Ile^{303} and Gly^{305} (the CBAL equivalent to Trp^{416} of MT-ACS1), Met^{310} and Asn^{311}, and the four-residue connector loop in between are all important for proper architecture of the aryl substrate binding pocket of CBAL (*27*).

The experimental evidence presented here clearly indicates that Trp^{416}, Val^{388}, Thr^{313}, and Ile^{312} form at least part of the acetate binding site of MT-ACS1. However, these cannot be the only residues that influence acyl substrate binding. In the *Pyrobaculum aerophilum* ACS (PA-ACS), all four of these residues are fully conserved (Figure 2), yet this enzyme can utilize a wider range of substrates than most ACSs (*29*). In addition to acetate and propionate, PA-ACS can also utilize butyrate and isobutyrate (2-methylpropionate) as substrates. Interestingly, PA-ACS was found to have higher activity with propionate than acetate at an acyl substrate concentration of 5 mM. Kinetic parameters were only determined using acetate as the acyl substrate. Thus, it is not clear whether this enzyme has a higher catalytic efficiency with acetate than propionate.

The molecular basis for the broader substrate range for PA-ACS is not clear. However, another archaeal ACS from *Archaeoglobus fulgidus* (AF-ACS2) also shows a broader substrate range and only a slight preference for acetate over propionate (*30*). As for PA-ACS, the four pocket residues identified in MT-ACS1 are fully conserved in the *A. fulgidus* enzyme. Several residues in AF-ACS2 and MT-ACS1 that reside near the acetate pocket identified herein are currently under investigation to determine the roles of other residues that influence acyl substrate utilization in ACS and the SACSs.

The most remarkable result from this study is that alteration of a single key residue within the acetate binding site could have such a dramatic effect of substrate selection. The ability of the Trp^{416}Gly variant to utilize a number of larger substrates in preference to acetate and to utilize branched-chain acyl substrates is most likely due not only to loss of the bulky Trp side chain but also to the increased flexibility in this region due to introduction of Gly. Additional changes in the active site are necessary for these substrates to be utilized well though, as the turnover rate suffered as the affinity for larger substrates increased. Finally, although alterations at each of these four residues influenced substrate selection, it is clear that these four residues alone do not define the acetate binding pocket and additional residues are involved.

REFERENCES

1. Anke, H., and Spector, L. B. (1975) Evidence for an acetyl-enzyme intermediate in the action of acetyl-CoA synthetase, *Biochem. Biophys. Res. Commun. 67*, 767−773.
2. Berg, P. (1956) Acyl adenylates: an enzymatic mechanism of acetate activation, *J. Biol. Chem. 222*, 991−1013.
3. Berg, P. (1956) Adenylates: the synthesis and properties of adenyl acetate, *J. Biol. Chem. 222*, 1015−1034.
4. Webster, L. T., Jr. (1963) Studies of the acetyl coenzyme A synthetase reaction. I. Isolation and characterization of enzyme-bound acetyl adenylate, *J. Biol. Chem. 238*, 4010−4015.
5. Chang, K. H., Xiang, H., and Dunaway-Mariano, D. (1997) Acyl-adenylate motif of the acyl-adenylate/thioester-forming enzyme superfamily: a site-directed mutagenesis study with the *Pseudomonas sp.* strain CBS3 4-chlorobenzoate:coenzyme A ligase, *Biochemistry 36*, 15650−15659.
6. An, J. H., Lee, G. Y., Jung, J. W., Lee, W., and Kim, Y. S. (1999) Identification of residues essential for a two-step reaction by malonyl-CoA synthetase from *Rhizobium trifolii*, *Biochem. J. 344* (Part 1), 159−166.
7. Horswill, A. R., and Escalante-Semerena, J. C. (2002) Characterization of the propionyl-CoA synthetase (PrpE) enzyme of *Salmonella enterica*: residue Lys592 is required for propionyl-AMP synthesis, *Biochemistry 41*, 2379−2387.
8. Lee, H. Y., Na, K. B., Koo, H. M., and Kim, Y. S. (2001) Identification of active site residues in *Bradyrhizobium japonicum* acetyl-CoA synthetase, *J. Biochem. (Tokyo) 130*, 807−813.
9. May, J. J., Kessler, N., Marahiel, M. A., and Stubbs, M. T. (2002) Crystal structure of DhbE, an archetype for aryl acid activating domains of modular nonribosomal peptide synthetases, *Proc. Natl. Acad. Sci. U.S.A. 99*, 12120−12125.
10. Stuible, H., Buttner, D., Ehlting, J., Hahlbrock, K., and Kombrink, E. (2000) Mutational analysis of 4-coumarate:CoA ligase identifies functionally important amino acids and verifies its close relationship to other adenylate-forming enzymes, *FEBS Lett. 467*, 117−122.
11. Conti, E., Franks, N. P., and Brick, P. (1996) Crystal structure of firefly luciferase throws light on a superfamily of adenylate-forming enzymes, *Structure 4*, 287−298.
12. Conti, E., Stachelhaus, T., Marahiel, M. A., and Brick, P. (1997) Structural basis for the activation of phenylalanine in the nonribosomal biosynthesis of gramicidin S, *EMBO J. 16*, 4174−4183.
13. Babbitt, P. C., Kenyon, G. L., Martin, B. M., Charest, H., Slyvestre, M., Scholten, J. D., Chang, K. H., Liang, P. H., and Dunaway-Mariano, D. (1992) Ancestry of the 4-chlorobenzoate dehalogenase: analysis of amino acid sequence identities among families of acyl:adenyl ligases, enoyl-CoA hydratases/isomerases, and acyl-CoA thioesterases, *Biochemistry 31*, 5594−5604.
14. Kleinkauf, H., and Von Dohren, H. (1996) A nonribosomal system of peptide biosynthesis, *Eur. J. Biochem. 236*, 335−251.
15. Marahiel, M. A., Stachelhaus, T., and Mootz, H. D. (1997) Modular peptide synthetases involved in nonribosomal peptide synthesis, *Chem. Rev. 97*, 2651−2674.
16. Gulick, A. M., Starai, V. J., Horswill, A. R., Homick, K. M., and Escalante-Semerena, J. C. (2003) The 1.75 Å crystal structure of acetyl-CoA synthetase bound to adenosine-5′-propylphosphate and coenzyme A, *Biochemistry 42*, 2866−2873.

17. Jogl, G., and Tong, L. (2004) Crystal structure of yeast acetyl-coenzyme A synthetase in complex with AMP, *Biochemistry 43*, 1425−1431.
18. Grayson, N. A., and Westkaemper, R. B. (1988) Stable analogs of acyl adenylates. Inhibition of acetyl- and acyl-CoA synthetase by adenosine 5′-alkylphosphates, *Life Sci. 43*, 437−444.
19. Altschul, S. F., Madden, T. L., Schaffer, A. A., Zhang, J., Zhang, Z., Miller, W., and Lipman, D. J. (1997) Gapped BLAST and PSI-BLAST: a new generation of protein database search programs, *Nucleic Acids Res. 25*, 3389−3402.
20. Altschul, S. F., Gish, W., Miller, W., Myers, E. W., and Lipman, D. J. (1990) Basic local alignment search tool, *J. Mol. Biol. 215*, 403−410.
21. Thompson, J. D., Gibson, T. J., Plewniak, F., Jeanmougin, F., and Higgins, D. J. (1997) The Clustal X windows interface: flexible strategies for multiple sequence alignment aided by quality analysis tools, *Nucleic Acids Res. 25*, 4876−4882.
22. Bradford, M. M. (1976) A rapid and sensitive method for the quantitation of microgram quantities of protein utilizing the principle of protein-dye binding, *Anal. Biochem. 72*, 248−254.
23. Lipmann, F., and Tuttle, L. C. (1945) A specific micromethod for determination of acyl phosphates, *J. Biol. Chem. 159*, 21−28.
24. Rose, I. A., Grunberg-Manago, M., Korey, S. F., and Ochoa, S. (1954) Enzymatic phosphorylation of acetate, *J. Biol. Chem. 211*, 737−756.
25. Fujino, T., Takei, Y. A., Sone, H., Ioka, R. X., Kamataki, A., Magoori, K., Takahashi, S., Sakai, J., and Yamamoto, T. T. (2001) Molecular identification and characterization of two medium-chain acyl-CoA synthetases, MACS1 and the Sa gene product, *J. Biol. Chem. 276*, 35961−35966.
26. Morgan-Kiss, R. M., and Cronan, J. E. (2004) The *Escherichia coli fadK* (*ydiD*) gene encodes an anerobically regulated short chain acyl-CoA synthetase, *J. Biol. Chem. 279*, 37324−37333.
27. Gulick, A. M., Lu, X., and Dunaway-Mariano, D. (2004) Crystal structure of 4-chlorobenzoate:CoA ligase/synthetase in the unliganded and aryl substrate-bound states, *Biochemistry 43*, 8670−8679.
28. Lindermayr, C., Fliegmann, J., and Ebel, J. (2003) Deletion of a single amino acid residue from different 4-coumarate:CoA ligases from soybean results in the generation of new substrate specificities, *J. Biol. Chem. 278*, 2781−2786.
29. Brasen, C., Urbanke, C., and Schonheit, P. (2005) A novel octameric AMP-forming acetyl-CoA synthetase from the hyperthermophilic crenarchaeon *Pyrobaculum aerophilum*, *FEBS Lett. 579*, 477−482.
30. Ingram-Smith, C., and Smith, K. S. (2006) AMP-forming acetyl-CoA synthetases in *Archaea* show unexpected diversity in substrate utilization. *Archaea* (in press).

BI061023E